第40卷 第2期 岩 石 矿 物 学 杂 志 Vol. 40, No. 2: 257~268
2021年3月 ACTA PETROLOGICA ET MINERALOGICA Mar., 2021

吉林中部敖花村角闪辉长岩锆石 U-Pb 定年、Hf 同位素和岩石地球化学特征

孙永刚[1,2],李碧乐[1],王永胜[2],李 良[3],张学海[2],赵昌吉[1],李翱鹏[2]

(1. 吉林大学 地球科学学院, 吉林 长春 130061; 2. 吉林省地质调查院, 吉林 长春 130102; 3. 云南大学 地球科学学院, 云南 昆明 650000)

摘 要: 古太平洋板块的俯冲在欧亚大陆东缘的区域构造演化中发挥了重要作用,但其发生的时间尚不清楚。本文报道了吉林中部新发现的敖花村角闪辉长岩的锆石 U-Pb 年龄、Hf 同位素组成和岩石地球化学数据。锆石 U-Pb 定年显示,角闪辉长岩形成于早侏罗世(180.3 ± 2.3 Ma),锆石 εHf(t)值高且均一(9.6~11.3)。岩石地球化学分析显示样品低 Si 和 Al,高 Fe、Mg 和 Ca,富集轻稀土和大离子亲石元素(如 Rb、Ba、U、K 和 Sr),亏损重稀土和高场强元素(如 Nb、Ta 和 Ti),具有弱 Eu 负异常(δEu = 0.67~0.98)。岩石起源于板片流体交代的亏损岩石圈地幔,形成过程中分离结晶、地壳混染和堆晶作用不明显。结合东北地区东段早中生代火成岩组合及时空分布,认为古太平洋板块向欧亚大陆下的俯冲开始于早侏罗世,敖花村角闪辉长岩形成于与古太平洋俯冲密切相关的弧后环境。

关键词: 吉林中部; 角闪辉长岩; 锆石 U-Pb 定年; 岩石地球化学; Hf 同位素组成; 古太平洋板块

中图分类号: P597$^+$.3; P595; P588.12$^+$4 **文献标识码**: A **文章编号**: 1000-6524(2021)02-0257-12

Zircon U-Pb dating, Hf isotopic and geochemical characteristics of the hornblende gabbro in Aohua Village, central Jilin Province

SUN Yong-gang[1,2], LI Bi-le[1], WANG Yong-sheng[2], LI Liang[3], ZHANG Xue-hai[2], ZHAO Chang-ji[1] and LI Ao-peng[2]

(1. College of Earth Sciences, Jilin University, Changchun 130061, China; 2. Geological Survey Institute of Jilin Province, Changchun 130102, China; 3. College of Earth Sciences, Yunnan University, Kunming 650000, China)

Abstract: The subduction of the Paleo-Pacific Plate played an important role in the regional tectonic evolution of the eastern margin of the Eurasian continent, but the timing of this event remains ambiguous. To address this issue, this paper reports zircon U-Pb ages, zircon Hf isotopic compositions and petrogeochemical data of whole-rocks for the newly-found hornblende gabbro in Aohua Village, central Jilin Province. Zircon U-Pb dating shows that the hornblende gabbro was formed in Early Jurassic (180.3 ± 2.3 Ma), and has high and uniform εHf(t) values (9.6~11.3). Petrogeochemical analyses show that the samples are characterized by low Si and Al, and high Fe, Mg, and Ca, enrichment of light rare earth elements and large-ion lithophile elements (e.g., Rb, Ba, U, K, and Sr), and depletion of heavy rare earth elements and high-field-strength elements (e.g., Nb, Ta, and Ti), and have weak negative Eu anomalies (δEu = 0.67~0.98). They were derived from a depleted lithospheric mantle source that had previously been metasomatized by slab-derived fluids, with unapparent effects of fractional crystallization, crustal contamination and cumulation in the formation process. Combined with rock associations and spatial distri-

收稿日期: 2020-10-31; **接受日期**: 2021-01-30; **编辑**: 尹淑苹

基金项目: 国家自然科学基金资助项目(41272093); 吉林省自然科学基金资助项目(20180101089JC)

作者简介: 孙永刚(1988-), 男, 博士研究生, 主要从事热液矿床成矿理论与预测研究, E-mail: xg429805791@163.com。

bution of Early Mesozoic igneous rocks in the eastern part of Northeast China, the authors hold that the subduction of the Paleo-Pacific Plate beneath the Eurasian continent started in Early Jurassic, and the hornblende gabbro was formed in the back-arc setting which might have been closely related to the subduction of the Paleo-Pacific Plate.

Key words: central Jilin Province; hornblende gabbro; zircon U-Pb dating; petrogeochemistry; Hf isotopic compositions; Paleo-Pacific Plate

Fund support: National Natural Science Foundation of China(41272093); Natural Science Foundation of Jilin Province(20180101089JC)

东北地区位于中亚造山带的最东段,自西向东由额尔古纳地块、兴安地块、松嫩地块、佳木斯地块和那丹哈达地体组成(图 1a; Wu *et al.*, 2011)。该地区不仅记录了古亚洲洋的最终闭合,而且记录了古太平洋板块向欧亚大陆下的俯冲作用(Tang *et al.*, 2018; Wang *et al.*, 2019)。但是古太平洋板块俯冲开始的时间仍有争议,大多数研究人员认为古太平洋板块的俯冲开始于早中侏罗世(孙德有等,2005; Wu *et al.*, 2007; 裴福萍等, 2008; Zhou *et al.*, 2009; Yu *et al.*, 2012; Xu *et al.*, 2013; Guo *et al.*, 2015),然而也有学者认为俯冲开始于三叠纪(赵春荆等, 1996; Wilde, 2015; Yang *et al.*, 2015),甚至是早二叠世(Ernst *et al.*, 2007; Sun *et al.*, 2015)。东北地区显生宙花岗岩类分布广泛,前人已经对这些花岗岩进行了大量的地质年代学和地球化学研究(葛茂卉等, 2020),但是花岗岩形成环境的多样性(Maniar and Piccoli, 1989)也造成了关于古太平洋板块俯冲开始时间的争议。基性侵入岩对于研究构造背景具有重要意义,但是东北地区基性侵入岩的地质年代学和岩石成因研究很少,这主要是因为基性侵入岩只零星出现,而且相对于花岗岩类的规模小很多(Yu *et al.*, 2012; Guo *et al.*, 2015;Wang *et al.*, 2017)。吉林省中部地区位于松嫩地块东缘,小兴安岭-张广才岭地区南部(图 1a),是研究古亚洲洋和环太平洋构造域叠加-过渡的理想场所。因此,本文选取吉林中部地区新发现的敖花村角闪辉长岩进行锆石 U-Pb 定年、Hf 同位素和岩石地球化学研究,对角闪辉长岩的形成时代、岩浆源区和构造背景进行了探讨,这些资料对于研究东北地区中生代构造背景和古亚洲洋向环太平洋构造域转变的时间具有重要意义。

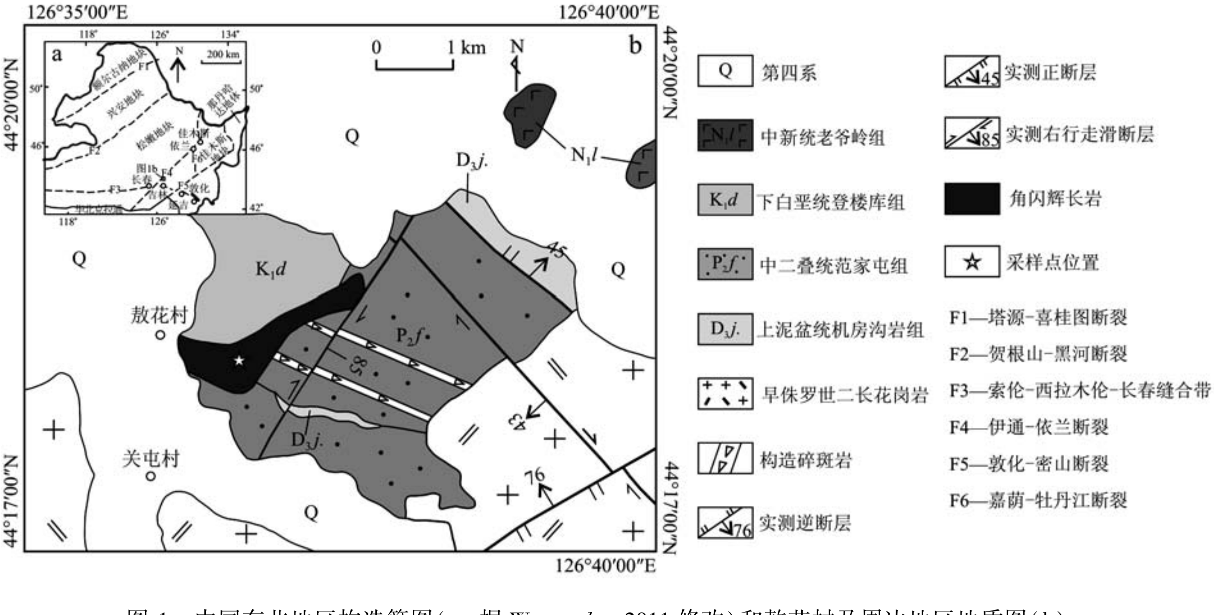

图 1 中国东北地区构造简图(a, 据 Wu *et al.*, 2011 修改)和敖花村及周边地区地质图(b)

Fig. 1 Tectonic setting map of Northeast China (a, modified after Wu *et al.*, 2011) and geological map of Aohua Village and its surrounding areas (b)

1　地质背景及样品描述

角闪辉长岩岩体主要出露在吉林省舒兰市敖花村附近,角闪辉长岩出露面积约 0.67 km^2,侵入到中二叠统范家屯组灰绿色变质细砂岩之中,北侧被下白垩统登楼库组灰-灰褐色含砾粗砂岩、粉砂岩不整合覆盖,西侧被第四系沉积物覆盖,北东侧被北东向右行走滑断层切割(图 1b)。角闪辉长岩的新鲜面呈灰黑色,辉长结构,块状构造。岩石主要成分为斜长石(45%~50%,体积分数)、辉石(25%~30%)和角闪石(20%~25%)(图 2)。

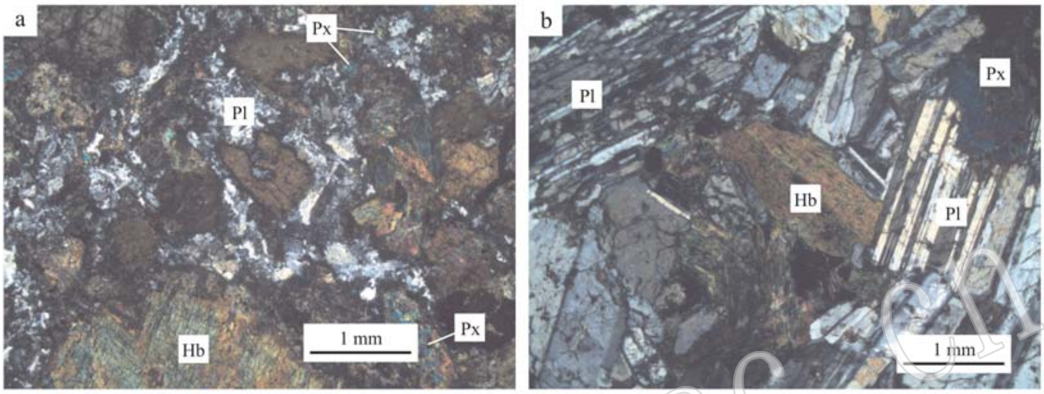

图 2　敖花村角闪辉长岩显微照片(+)

Fig. 2　Microphotographs of the hornblende gabbro in Aohua Village(+)

Pl—斜长石; Hb—角闪石; Px—辉石

Pl—plagioclase; Hb—hornblende; Px—pyroxene

2　分析方法

锆石的分选、制靶和 CL 图像的采集均在廊坊市尚艺岩矿检测技术服务有限公司完成,将分选好的锆石置于双目镜下,选择无裂隙、透明、无包裹体的锆石颗粒,将其制成环氧树脂样品靶。LA-ICP-MS 锆石 U-Pb 同位素定年在北京燕都中实测试技术有限公司完成,激光剥蚀系统为 New Wave UP213, ICP-MS 为德国耶拿 M90。测试剥蚀光斑直径为 30 μm,频率为 10 Hz,能量密度约为 2.5 J/cm^2。采用锆石标准 91500 作为外标进行同位素分馏校正,每分析 12 个样品点,分析 2 次 91500,并分析 1 次 Plěsovice 标样作为监控。数据处理采用 GLITTER 4.0 完成,锆石 U-Pb 谐和及加权年龄的计算采用 ISOPLOT 3.0 完成。

全岩主微量和稀土元素的测试在北京燕都中实测试技术有限公司完成,先将岩石粗碎至厘米级,选取新鲜样品用纯化水洗净,烘干、粉碎至 200 目以备测试使用。主量元素测试先将粉末样品称量后加 $Li_2B_4O_7$(1∶8)助熔剂混合,利用融样机加热至 1 150 ℃,使其在铂金坩埚中熔融成均一玻璃片体,再使用 XRF(Zetium, Panalytical)测试,测试结果误差小于 1%。全岩的 Fe_2O_3 和 FeO 含量分别采用磺基水杨酸光度法和重铬酸钾溶液滴定法测定。微量元素测试先将 200 目粉末样品称量并置放入聚四氟乙烯溶样罐并加入 HF+HNO_3,在干燥箱中将高压消解罐保持在 190 ℃温度 72 h,后取出经过赶酸并将溶液定容为稀溶液上机测试。使用 ICP-MS(M90, Analytikjena)完成,所测数据根据监控标样 GSR-2 显示误差小于 5%,部分挥发性元素及极低含量元素的分析误差小于 10%。

锆石原位 Lu-Hf 同位素测试在北京燕都中实测试技术有限公司完成,仪器为美国热电 Neptune-plus MC-ICP-MS 与激光烧蚀进样系统 New Wave UP213。测试步骤与校准方法类似于 Wu 等(2006),锆石剥蚀使用频率为 8 Hz,能量为 16 J/cm^2 的激光剥蚀 31 s,剥蚀出直径约 30 μm 的剥蚀坑,测试时,由于锆石中的 $^{176}Lu/^{177}Hf$ 值极低(一般 <0.002), ^{176}Lu 对 ^{176}Hf 的同位素干扰可以忽略不计,每个测试点的 $^{173}Yb/^{172}Yb$ 平均值用于计算 Yb 的分馏系数,然后再扣除 ^{176}Yb 对 ^{176}Hf 的同质异位素干扰。$^{173}Yb/^{172}Yb$ 的同位素比值为 1.352 74。

3 分析结果

3.1 LA-ICP-MS 锆石 U-Pb 定年

敖花村角闪辉长岩中的锆石普遍具有岩浆振荡环带,锆石晶体长轴 130~230 μm,短轴 80~170 μm,多呈半自形-它形,锆石的边部出现港湾状的外形特征,溶蚀结构明显,极可能是受到了热液蚀变作用的影响。但是本次研究只选取未受到热液蚀变作用影响的锆石晶域进行 U-Pb 定年(图 3),因此同样可以得到原岩的形成年龄(Liati *et al.*, 2002; Tomaschek *et al.*, 2003)。

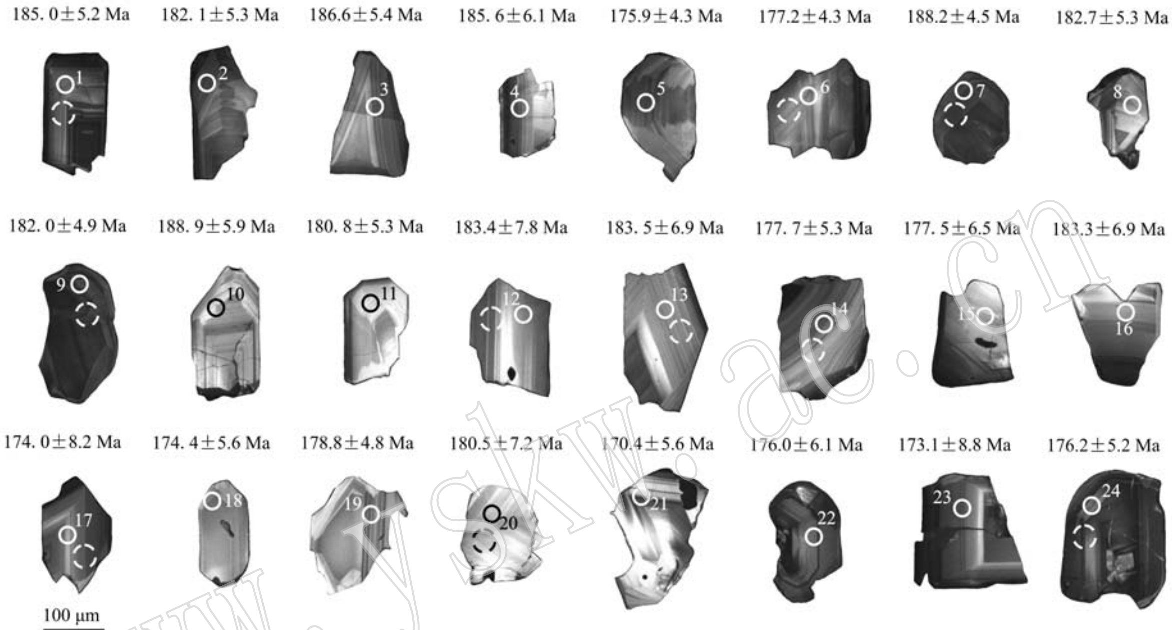

图 3 敖花村角闪辉长岩锆石 CL 图像(实线圆圈为 U-Pb 定年位置,虚线圆圈为 Lu-Hf 同位素分析位置)

Fig. 3 Cathodoluminescence (CL) images of zircons from the hornblende gabbro in Aohua Village(the solid and dashed circles represent spots for U-Pb and Lu-Hf analysis, respectively)

锆石 24 个测试点的 Th 和 U 的含量分别为 57.82×10^{-6}~947.78×10^{-6} 和 61.82×10^{-6}~$1\ 091.64\times10^{-6}$,Th/U 值为 0.61~1.74(表 1),均大于 0.10,表明该组锆石为岩浆成因的锆石(Wu and Zheng, 2004)。基性-超基性岩由于 Si 含量低(SiO_2<53%),而且 Zr 含量相比中酸性岩低,导致基性-超基性岩中锆石($ZrSiO_4$)的含量较少,但是通过增加用于锆石分选的基性-超基性岩石样品量,可以最大限度地规避这一问题。国内外近年来也有大量关于基性-超基性岩可靠的锆石成岩年龄数据相继发表(Yu *et al.*, 2012; 王冠等, 2014; 奥琮等, 2015; Guo *et al.*, 2015; 刘金龙等, 2016; 闫佳铭等, 2016; Zhao *et al.*, 2019; 葛茂卉等, 2020; Sun *et al.*, 2020; Yan *et al.*, 2020)。本次研究采集大量的角闪辉长岩样品进行锆石分选,得到 24 个测试点的 $^{206}Pb/^{238}U$ 加权平均年龄为 180.3 ± 2.3 Ma(图 4b),代表敖花村角闪辉长岩的结晶年龄,属于早侏罗世。

3.2 岩石地球化学特征

敖花村角闪辉长岩具有低 Si 和 Al,高 Fe、Mg 和 Ca 的特点。样品 SiO_2 含量为 45.02%~47.58%,Al_2O_3 含量为 12.26%~13.69%,$^{T}Fe_2O_3$ 含量为 11.20%~13.74%,MgO 含量为 11.32%~15.13%,CaO 含量为 7.34%~9.65%,TiO_2 含量为 0.65%~1.30%(表 2)。

敖花村角闪辉长岩的 ΣREE 为 46.95×10^{-6}~72.37×10^{-6},Eu 具弱负异常(δEu = 0.67~0.98)。LREE/HREE = 4.96~5.97,$(La/Yb)_N$ 值为 4.37~5.70,轻稀土元素富集,重稀土元素亏损,稀土元素配分曲线表现为明显右倾(图 5a)。原始地幔标准化微量元素蛛网图中显示(图 5b),敖花村角闪辉长岩样品富集大离子亲石元素(如 Rb、Ba、U、K 和 Sr),亏损高场强元素(如 Nb、Ta 和 Ti)和 P 元素。

表 1　敖花村角闪辉长岩锆石 U-Pb 同位素定年数据

Table 1　Zircon U-Pb isotopic dating results of the hornblende gabbro in Aohua Village

测点号	$w_B/10^{-6}$			Th/U	同位素比值				年龄/Ma			
	Pb	Th	U		$^{207}Pb/^{235}U$	1σ	$^{206}Pb/^{238}U$	1σ	$^{207}Pb/^{235}U$	1σ	$^{206}Pb/^{238}U$	1σ
AHC-N1-01	40.41	947.78	1091.64	0.87	0.201 39	0.011 26	0.029 11	0.000 83	186.3	9.5	185.0	5.2
AHC-N1-02	10.26	181.02	289.22	0.63	0.199 51	0.012 77	0.028 65	0.000 84	184.7	10.8	182.1	5.3
AHC-N1-03	8.11	137.07	224.29	0.61	0.201 07	0.017 56	0.029 37	0.000 87	186.0	14.8	186.6	5.4
AHC-N1-04	8.54	181.92	223.61	0.81	0.199 57	0.020 22	0.029 21	0.000 98	184.8	17.1	185.6	6.1
AHC-N1-05	8.47	237.23	212.81	1.11	0.186 31	0.029 73	0.027 67	0.000 68	173.5	25.5	175.9	4.3
AHC-N1-06	6.79	186.41	163.56	1.14	0.192 19	0.025 07	0.027 86	0.000 68	178.5	21.4	177.2	4.3
AHC-N1-07	17.92	427.72	432.83	0.99	0.205 87	0.019 99	0.029 63	0.000 72	190.1	16.8	188.2	4.5
AHC-N1-08	5.52	92.89	153.09	0.61	0.200 38	0.018 95	0.028 75	0.000 84	185.5	16.0	182.7	5.3
AHC-N1-09	22.82	880.96	506.16	1.74	0.196 97	0.009 83	0.028 64	0.000 78	182.6	8.3	182.0	4.9
AHC-N1-10	4.55	86.41	105.11	0.82	0.204 77	0.050 13	0.029 73	0.000 94	189.2	42.3	188.9	5.9
AHC-N1-11	3.58	76.67	100.52	0.76	0.196 93	0.028 30	0.028 45	0.000 84	182.5	24.0	180.8	5.3
AHC-N1-12	8.46	215.81	200.07	1.08	0.196 09	0.032 65	0.028 85	0.001 24	181.8	27.7	183.4	7.8
AHC-N1-13	5.65	163.58	143.58	1.14	0.193 95	0.031 07	0.028 87	0.001 10	180.0	26.4	183.5	6.9
AHC-N1-14	5.22	95.33	148.53	0.64	0.192 78	0.022 06	0.027 95	0.000 84	179.0	18.8	177.7	5.3
AHC-N1-15	5.60	118.20	152.68	0.77	0.188 50	0.020 86	0.027 92	0.001 04	175.4	17.8	177.5	6.5
AHC-N1-16	2.62	57.82	61.82	0.94	0.196 74	0.061 00	0.028 84	0.001 10	182.4	51.8	183.3	6.9
AHC-N1-17	5.29	167.89	137.49	1.22	0.188 92	0.032 11	0.027 36	0.001 31	175.7	27.4	174.0	8.2
AHC-N1-18	7.46	211.13	195.44	1.08	0.189 10	0.024 34	0.027 42	0.000 89	175.9	20.8	174.4	5.6
AHC-N1-19	5.88	164.23	150.85	1.09	0.192 57	0.019 82	0.028 13	0.000 76	178.8	16.9	178.8	4.8
AHC-N1-20	3.24	93.89	78.00	1.20	0.195 38	0.039 04	0.028 40	0.001 14	181.2	33.2	180.5	7.2
AHC-N1-21	9.88	330.95	254.70	1.30	0.183 32	0.022 14	0.026 78	0.000 90	170.9	19.0	170.4	5.6
AHC-N1-22	9.73	261.18	262.69	0.99	0.188 83	0.014 41	0.027 67	0.000 97	175.6	12.3	176.0	6.1
AHC-N1-23	19.78	539.02	509.87	1.06	0.187 74	0.016 82	0.027 21	0.001 40	174.7	14.4	173.1	8.8
AHC-N1-24	16.43	405.53	436.34	0.93	0.189 77	0.012 63	0.027 71	0.000 83	176.4	10.8	176.2	5.2

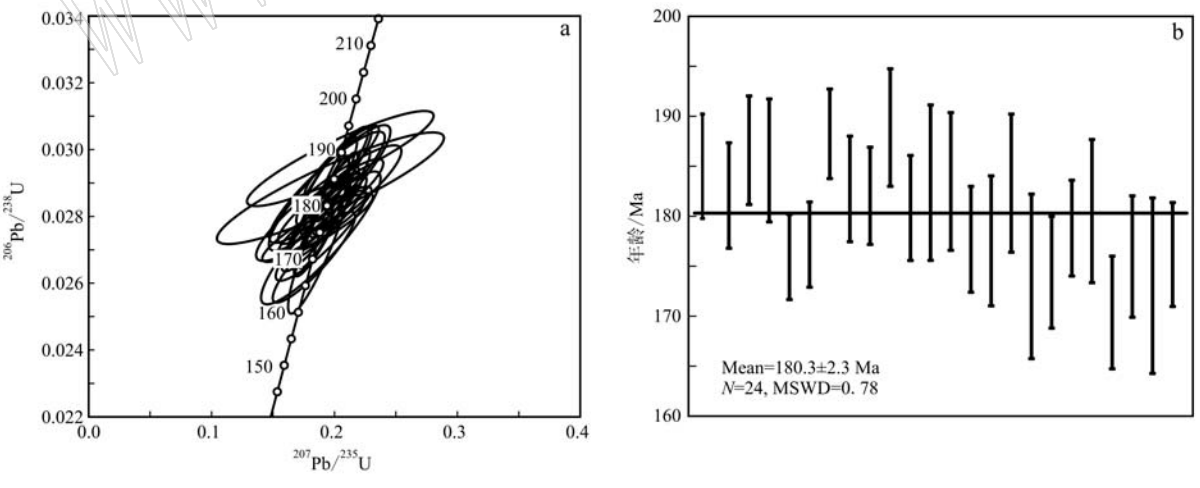

图 4　敖花村角闪辉长岩锆石 U-Pb 年龄谐和图(a)和加权平均年龄图(b)

Fig. 4　Concordia diagram (a) and weighted average ages diagram (b) showing zircon U-Pb dating result of the hornblende gabbro in Aohua Village

3.3　锆石 Hf 同位素

敖花村角闪辉长岩样品中锆石的 $^{176}Hf/^{177}Hf$ 值为 0.282 932~0.282 980，$\varepsilon Hf(t)$ 值为 9.6~11.3，测试点均投在球粒陨石演化线和亏损地幔演化线之间(图 6)，锆石 Hf 同位素单阶段模式年龄(t_{DM1})为 447~381 Ma，二阶段模式年龄(t_{DM2})为 612~504 Ma(表 3)。

表 2 敖花村角闪辉长岩样品主量元素($w_B/\%$)、稀土元素和微量元素($w_B/10^{-6}$)含量及有关参数

Table 2 Major ($w_B/\%$), REE and trace element ($w_B/10^{-6}$) content and parameters of the hornblende gabbro in Aohua Village

样品号	AHC-YQ1	AHC-YQ2	AHC-YQ3	AHC-YQ4	AHC-YQ5	AHC-YQ6
SiO_2	47.58	45.02	46.24	46.54	46.22	45.35
TiO_2	1.30	1.02	0.74	0.78	0.65	0.70
Al_2O_3	12.75	13.69	12.26	12.69	12.69	12.37
FeO	6.48	7.74	2.03	1.48	8.04	8.83
Fe_2O_3	4.70	5.23	9.18	9.73	2.36	2.23
MnO	0.15	0.17	0.21	0.21	0.22	0.22
MgO	11.32	11.68	15.13	14.18	15.01	14.94
CaO	9.65	8.26	7.59	7.96	7.34	8.38
Na_2O	2.44	1.73	1.49	1.29	1.53	1.16
K_2O	0.68	1.07	1.15	1.30	1.05	0.84
P_2O_5	0.13	0.13	0.16	0.17	0.11	0.16
LOI	2.52	3.36	3.15	3.07	4.36	4.16
TOTAL	99.71	99.11	99.33	99.40	99.58	99.34
$Mg^{\#}$	65.5	62.7	72.4	71.2	72.6	71.2
Be	0.66	0.63	0.72	0.49	0.77	0.61
Cr	262	293	332	360	342	370
Rb	19.39	28.15	40.20	41.90	35.80	27.60
Sr	696	556	241	360	252	298
Y	14.21	9.19	17.60	16.00	12.40	13.60
Zr	99.30	135.68	94.00	84.50	79.70	75.20
Nb	3.03	4.39	6.53	5.94	5.13	5.46
Cs	2.00	3.38	2.40	3.75	2.77	2.47
Ba	190	227	288	287	263	223
La	10.46	7.41	11.40	12.00	10.50	11.00
Ce	23.23	16.75	26.90	25.20	28.00	24.90
Pr	3.15	2.27	3.21	3.58	2.96	3.01
Nd	14.38	10.50	14.50	14.90	12.70	13.40
Sm	3.28	2.32	3.46	4.00	3.20	3.17
Eu	1.03	0.63	0.76	0.88	0.75	0.68
Gd	3.00	2.13	2.85	2.87	3.65	2.63
Tb	0.50	0.38	0.58	0.48	0.43	0.45
Dy	2.86	2.02	3.58	3.39	2.75	2.68
Ho	0.56	0.38	0.70	0.65	0.57	0.54
Er	1.50	0.97	2.07	1.79	1.38	1.41
Tm	0.23	0.16	0.32	0.27	0.23	0.21
Yb	1.43	0.92	1.76	1.42	1.26	1.30
Lu	0.20	0.13	0.28	0.23	0.18	0.19
Hf	3.05	1.76	3.02	2.86	2.83	2.76
Ta	0.19	0.26	0.16	0.14	0.15	0.15
Th	1.86	2.05	3.40	2.73	2.66	2.74
U	0.37	0.46	1.06	0.71	0.69	0.79
δEu	0.98	0.85	0.72	0.76	0.67	0.70
LREE	55.52	39.86	60.23	60.56	58.11	56.16
HREE	10.29	7.09	12.14	11.10	10.45	9.41
ΣREE	65.81	46.95	72.37	71.66	68.56	65.57
LREE/HREE	5.40	5.62	4.96	5.46	5.56	5.97
$(La/Yb)_N$	4.94	5.41	4.37	5.70	5.62	5.70

4 讨论

4.1 分离结晶、地壳混染和堆晶作用

敖花村角闪辉长岩地球化学成分的变化范围相对有限,再加上其高的 $Mg^{\#}$ 值(62.7~72.6)和 Cr 含量($262\times10^{-6}\sim370\times10^{-6}$),表明其母岩浆经历了非常有限的分离结晶作用(Zhang *et al.*, 2015)。角闪辉长岩同样没有经历明显的地壳混染,证据如下:① 样品的 Lu/Yb 值低且恒定(0.14~0.16),类似于幔源岩浆的范围(0.14~0.15),却低于陆壳岩浆范围(0.16~0.18)(Sun and McDonough, 1989);② 地壳物质明显富集 Zr 和 Hf,因此地壳混染会使 Zr 和 Hf 富集,但是角闪辉长岩样品并没有显示明显的 Zr 和 Hf 正异常(图 5b);③ 样品中没有地壳捕虏体或捕获晶,表明没有或很少发生地壳混染。另外,角闪辉长岩的堆晶作用也不明显,证据如下:① Eu 在斜长石中非常富集,但敖花村角闪辉长岩具有弱的负 Eu 异常(冯光英等, 2018; 杨泽黎等, 2018);② 角闪辉长岩岩体不发育堆晶层理(图略),同样镜下也并未见到典型的堆晶结构(图 2);③ 在 AFM 图解(图 7)中,样品均位于镁铁质-超镁铁质堆晶岩区域之外。

综上,分离结晶、地壳混染和堆晶作用对敖花村角闪辉长岩的形成贡献不大,所以可以利用它的地球化学组成来研究其岩浆源区。

4.2 岩浆源区

基性-超基性岩通常起源于岩石圈地幔或软流圈地幔(Cai *et al.*, 2012; Yan *et al.*, 2019)。敖花村角闪辉长岩富集 LILEs 和 LREEs,亏损 HFSEs(Nb、Ta、Zr 和 Hf),与亲岛弧的玄武岩相似,明显不同于来自软流圈地幔的正常型洋中脊玄武岩(N-MORB)(图 5a; Pearce *et al.*, 1984; Crawford *et al.*, 1987; Davidson, 1987)。角闪辉长岩样品较高的 La/Nb 值(1.69~3.45)和 La/Ta 值(28.7~85.7)也表明其来源于岩石圈地幔(La/Nb>1, La/Ta>20; Fitton *et al.*, 1988; Thompson and Morrison, 1988)而非软流圈地幔(La/Nb<1, La/Ta≈10; Fitton *et al.*, 1988; Thompson and Morrison, 1988)。此外,在 Th/Yb-Nb/Yb 图解(图 8a)中,角闪辉长岩样品的数据投影于 MORB-OIB 阵列之上,位于俯冲改造的岩石圈地幔起源的原始镁铁质熔体数据区域,表明它们的源区经历了俯冲交代作用(Sun *et al.*, 2020)。通过 Th/

表 3　敖花村角闪辉长岩锆石 Lu-Hf 同位素组成

Table 3　Zircon Lu-Hf isotopic compositions of the hornblende gabbro in Aohua Village

测点号	t /Ma	$^{176}Yb/^{177}Hf$	2σ	$^{176}Lu/^{177}Hf$	2σ	$^{176}Hf/^{177}Hf$	2σ	$\varepsilon Hf(0)$	$\varepsilon Hf(t)$	t_{DM1}	t_{DM2}	$f_{Lu/Hf}$
AHC-N1-01	180.0	0.024 220	0.000 074	0.000 831	0.000 002	0.282 948	0.000 025	6.2	10.1	428	578	−0.97
AHC-N1-02	180.0	0.031 422	0.000 276	0.001 077	0.000 009	0.282 937	0.000 025	5.8	9.7	447	606	−0.97
AHC-N1-03	180.0	0.024 240	0.000 203	0.000 773	0.000 004	0.282 972	0.000 019	7.1	11.0	394	524	−0.98
AHC-N1-04	180.0	0.030 100	0.000 184	0.000 956	0.000 004	0.282 956	0.000 020	6.5	10.3	419	562	−0.97
AHC-N1-05	180.0	0.008 165	0.000 122	0.000 269	0.000 005	0.282 932	0.000 024	5.7	9.6	445	612	−0.99
AHC-N1-06	180.0	0.026 738	0.000 356	0.000 864	0.000 008	0.282 943	0.000 020	6.1	9.9	435	589	−0.97
AHC-N1-07	180.0	0.019 375	0.000 077	0.000 625	0.000 003	0.282 980	0.000 021	7.4	11.3	381	504	−0.98
AHC-N1-08	180.0	0.018 979	0.000 284	0.000 612	0.000 010	0.282 934	0.000 021	5.8	9.6	445	608	−0.98
AHC-N1-09	180.0	0.020 069	0.000 247	0.000 721	0.000 010	0.282 953	0.000 020	6.4	10.3	421	568	−0.98
AHC-N1-10	180.0	0.019 565	0.000 084	0.000 633	0.000 003	0.282 957	0.000 022	6.6	10.4	413	556	−0.98

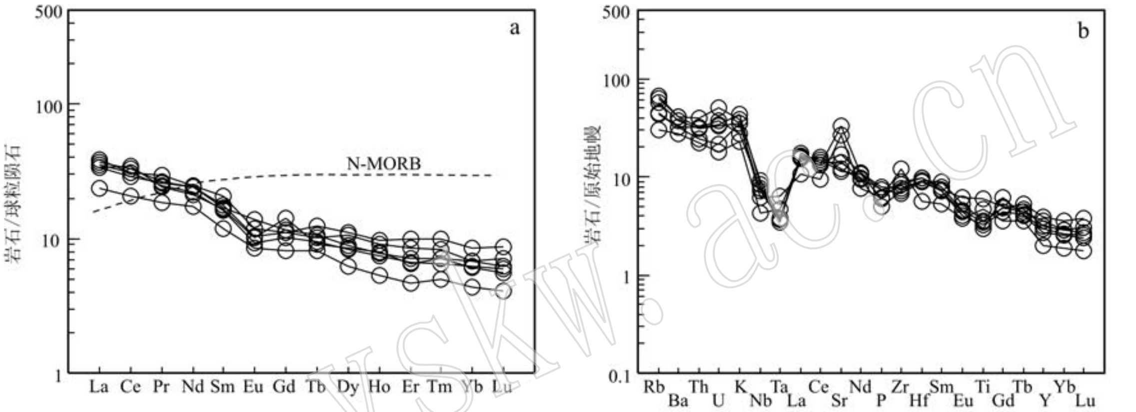

图 5　敖花村角闪辉长岩稀土元素球粒陨石标准化配分曲线(a, 球粒陨石标准化值据 Boynton, 1984; N-MORB 值据 Sun and Mcdonough, 1989)和微量元素原始地幔标准化蛛网图(b, 原始地幔标准化值据 Sun and Mcdonough, 1989)

Fig. 5　Chondrite-normalized REE patterns (a, chondrite-normalized values after Boynton, 1984; N-MORB values after Sun and McDonough, 1989) and primitive-mantle normalized trace elements spider diagram (b, primitive-mantle normalized values after Sun and Mcdonough, 1989) for the hornblende gabbro in Aohua Village

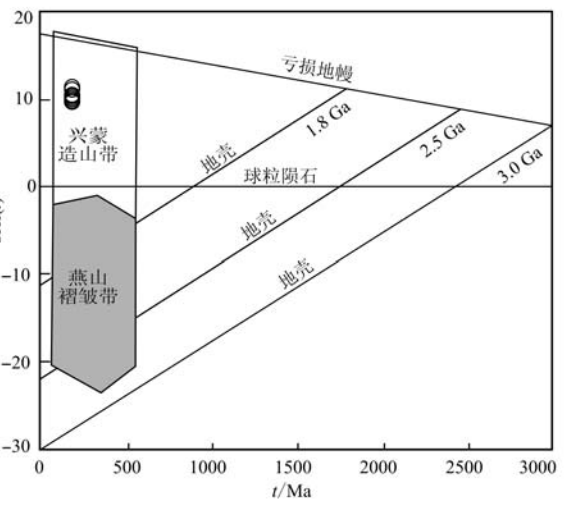

图 6　敖花村角闪辉长岩锆石 Hf 同位素图解(兴蒙造山带和燕山褶皱带数据据 Yang *et al.*, 2006)

Fig. 6　Zircon Hf isotopic diagram for the hornblende gabbro in Aohua Village (data for Xing-Meng Orogenic Belt and Yanshan Fold-Thrust Belt after Yang *et al.*, 2006)

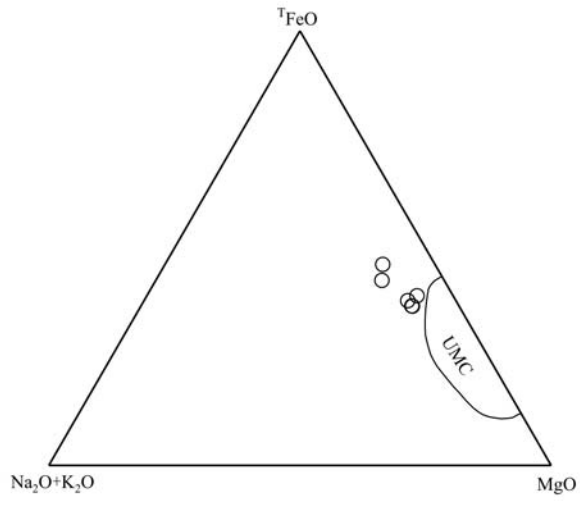

图 7　敖花村角闪辉长岩 AFM 图解(据 Coleman, 1977)

Fig. 7　AFM diagram for the hornblende gabbro in Aohua Village (after Coleman, 1977)

UMC—镁铁质-超镁铁质堆晶岩

UMC—mafic-ultramafic cumulates

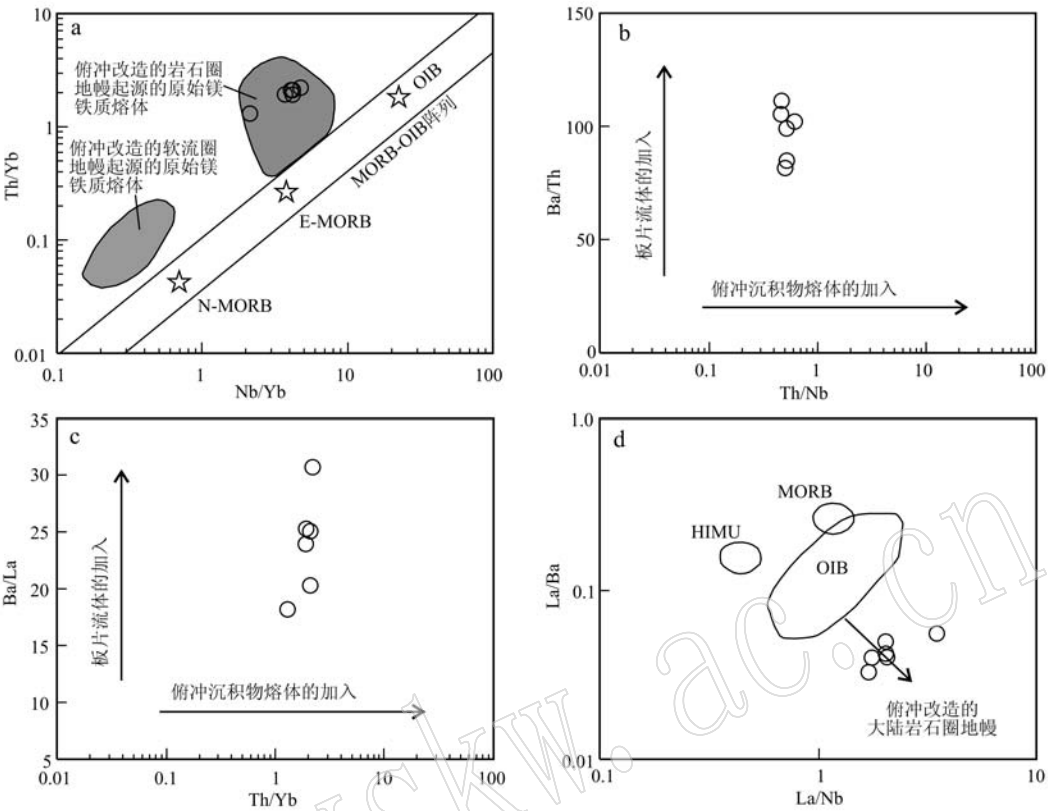

图 8 敖花村角闪辉长岩 Th/Yb - Nb/Yb(a, 底图据 Pearce, 2008; 俯冲改造的岩石圈和软流圈地幔起源的原始镁铁质熔体数据据 Leat *et al.*, 2002)、Ba/Th - Th/Nb(b, 据 Hanyu *et al.*, 2006)、Ba/La - Th/Yb(c, 据 Hanyu *et al.*, 2006)和 La/Ba - La/Nb(d, 据 Saunders *et al.*, 1992)图解

Fig. 8 Th/Yb - Nb/Yb(a, after Pearce, 2008; data for primitive mafic melts derived from subduction-modified lithospheric and asthenospheric mantle after Leat *et al.*, 2002), Ba/Th - Th/Nb(b, after Hanyu *et al.*, 2006), Ba/La - Th/Yb(c, after Hanyu *et al.*, 2006) and La/Ba - La/Nb(d, after Saunders *et al.*, 1992) diagrams of the hornblende gabbro in Aohua Village

N-MORB—正常型洋中脊玄武岩; E-MORB—富集型洋中脊玄武岩; OIB—洋岛玄武岩; HIMU—高 U/Pb 地幔

N-MORB—normal mid-ocean ridge basalt; E-MORB—enriched mid-ocean ridge basalt; OIB—ocean island basalt; HIMU—high U/Pb mantle source

Nb、Ba/Th、Th/Yb 和 Ba/La 值可以有效地识别俯冲沉积物熔体和板片流体。在 Ba/Th - Th/Nb 和 Ba/La - Th/Yb 图解中(图 8b、8c),角闪辉长岩样品显示源区经历了板片流体的改造。而且,样品中存在大量角闪石(20%~25%),由于角闪石等含水矿物只有在水达到饱和的情况下才结晶(Botcharnikov *et al.*, 2008),也说明原始岩浆的含水量较高(Ridolfi *et al.*, 2010),与流体交代地幔源区的特征一致(图 8b,c)。在 La/Ba - La/Nb 图解(图 8d)中,角闪辉长岩呈现出向大陆岩石圈地幔区域靠拢的趋势,同样暗示其岩石圈地幔源区。对于地幔来源的玄武质岩石而言,如果锆石 Hf 同位素模式年龄(t_{DM1})与其形成年龄相近,表明该岩石来源于亏损地幔(吴福元等, 2007),而且来源于亏损地幔的玄武质岩石通常具有高的 εHf(*t*)值(>10; Zhong *et al.*, 2017; Yan *et al.*, 2019)。敖花村角闪辉长岩的锆石 εHf(*t*)值高且均一(9.6~11.3; 表 3),锆石 Hf 同位素模式年龄(t_{DM1})为 447~381 Ma,与锆石结晶年龄相近,显示其亏损地幔特征。

综上所述,笔者认为敖花村角闪辉长岩起源于板片流体交代的亏损岩石圈地幔。

4.3 构造背景

敖花村角闪辉长岩的源区受到大洋板片俯冲流体的改造,但是俯冲板片流体的来源无法确定,因为小兴安岭-张广才岭地区的岩石圈地幔经历了俯冲板片流体或沉积物熔体的多次改造(Yu *et al.*, 2012)。东北地区显生宙构造演化主要受控于古亚洲洋俯冲和随后的古太平洋板块俯冲叠加(Meng *et* *al*., 2011; Wu *et al*., 2011; Xu *et al*., 2013; 郭锋, 2016)。那么敖花村角闪辉长岩的形成具体是受古亚洲洋还是古太平洋的影响,东北地区东段早中生代火成岩组合及时空分布是讨论这一问题的关键。

东北地区东段晚三叠世火成岩主要分布于索伦-西拉木伦-长春缝合带两侧,构成东西向火成岩带(Xu *et al*., 2013; Tang *et al*., 2018),构成双峰式火成岩组合(Cao *et al*., 2013; Xu *et al*., 2013; Wang *et al*., 2015; Tang *et al*., 2018)。而且,华北克拉通北缘东段及其邻近的缝合带上均缺失 240~225 Ma 的沉积作用,但普遍发育晚三叠世磨拉石建造,表明该地区已从造山隆起演化为造山后伸展环境(Liu *et al*., 2017; Tang *et al*., 2018; Wang *et al*., 2018)。因此,东北地区东段晚三叠世岩浆活动形成于与古亚洲洋最终闭合有关的造山后伸展环境,与古太平洋板块的俯冲无关。

Yu 等(2012)报道了小兴安岭-张广才岭地区早侏罗世(186~182 Ma)南北向镁铁质侵入岩带,这些镁铁质岩石产于与古太平洋俯冲密切相关的弧后环境,来源于受俯冲流体交代的地幔楔部分熔融,本次的研究也证实了这一岩浆源区。另外,延边地区早侏罗世(188~173 Ma)镁铁质侵入岩同样显示出与古太平洋板块俯冲相关的元素和同位素特征,是由俯冲沉积物熔体交代亏损地幔楔而形成的(Guo *et al*., 2015; Zhao *et al*., 2019)。空间上,延边地区早侏罗世镁铁质侵入体代表了南北向镁铁质弧岩浆带的南部范围(Zhao *et al*., 2019)。值得注意的是,这一南北向镁铁质侵入岩带近平行于欧亚大陆东缘、近垂直于当时古太平洋板块的运动方向(Engebretson *et al*., 1985)。因此,东北地区东段早侏罗世镁铁质侵入岩极有可能记录了古太平洋俯冲作用的开始。与古太平洋板块俯冲有关的早侏罗世增生杂岩已在欧亚大陆的东缘广泛发现(Fukuyama *et al*., 2013; Safonova and Santosh, 2014),也支持了这一观点。而且,吉黑东部发育早中侏罗世辉长岩、闪长岩、花岗闪长岩、二长花岗岩和正长花岗岩的侵入岩组合(Tang *et al*., 2016; Ma *et al*., 2017; Wang *et al*., 2017),与活动大陆边缘环境中的岩石组合一致(Miyashiro, 1974; Ewart, 1982; Barbarin,1999)。这些岩石属于钙碱性系列,富集 LILEs 和亏损 HFSEs(Tang *et al*., 2016; Ma *et al*., 2017; Wang *et al*., 2017),微量元素显示典型的弧岩浆作用特征,亦表明这些岩石均形成于与俯冲作用有关的活动大陆边缘环境中(Gill, 1981; Wilson, 1989)。因此,笔者认为吉黑东部早-中侏罗世岩浆事件与古太平洋板块俯冲到欧亚大陆之下有关。这一解释也得到了小兴安岭-张广才岭地区同时代双峰世火成岩和 A 型花岗岩的支持,该套岩石组合无疑代表了伸展的构造环境,东北地区东段的早-中侏罗世火成岩自东向西由活动大陆边缘的钙碱性组合到陆内伸展组合发生变化,对此最好的解释就是古太平洋板块早侏罗世向西俯冲到欧亚大陆之下,小兴安岭-张广才岭地区包括镁铁质侵入岩在内的双峰世火成岩和 A 型花岗岩是在俯冲的弧后背景下形成的(Yu *et al*., 2012; Xu *et al*., 2013)。

5　结论

(1) 锆石 LA-ICP-MS U-Pb 同位素年代学研究表明敖花村角闪辉长岩的加权平均年龄为 180.3 ± 2.3 Ma,形成于早侏罗世。

(2) 敖花村角闪辉长岩低 Si 和 Al,富 Fe、Mg 和 Ca,其锆石 εHf(t)值高且均一(9.6~11.3),它的形成过程中分离结晶、地壳混染和堆晶作用不明显,起源于板片流体交代的亏损岩石圈地幔。

(3) 古太平洋板块向西俯冲到欧亚大陆之下开始于早侏罗世,敖花村角闪辉长岩形成于与古太平洋俯冲密切相关的弧后环境。

References

Ao Cong, Sun Fengyue, Li Bile, *et al*. 2015. U-Pb dating, geochemistry and tectonic implications of Xiaojianshan gabbro in Qimantage Mountain, Eastern Kunlun Orogenic Belt[J]. Geotectonica et Metallogenia, 39(6): 1 176~1 184(in Chinese with English abstract).

Barbarin B. 1999. A review of the relationships between granitoid types, their origins and their geodynamic environments[J]. Lithos, 46(3): 605~626.

Botcharnikov R E, Almeev R R, Koepke J, *et al*. 2008. Phase relations and liquid lines of descent in hydrous ferrobasalt: Implications for the Skaergaard intrusion and Columbia River flood basalts[J]. Journal of Petrology, 49(9): 1 687~1 727.

Boynton W V. 1984. Cosmochemistry of the rare earth elements: Meteorite studies[A]. Henderson P. Rare Earth Element Geochemistry: Development in Geochemistry[C]. Amsterdam: Elsevier, 63~114.

Cai K D, Sun M, Yuan C, *et al*. 2012. Keketuohai mafic-ultramafic complex in the Chinese Altai, NW China: Petrogenesis and geodynamic significance[J]. Chemical Geology, 294~295: 26~41.

Cao H H, Xu W L, Pei F P, *et al*. 2013. Zircon U-Pb geochronology and petrogenesis of the Late Paleozoic-Early Mesozoic intrusive rocks in the eastern segment of the northern margin of the North China Block[J]. Lithos, 170~171: 191~207.

Coleman R G. 1977. Ophiolites[M]. Berlin, Heidelberg, New York: Springer-Verlag, 1~229.

Crawford A J, Falloon T J and Eggins S. 1987. The origin of island arc high-alumina basalts[J]. Contributions to Mineralogy and Petrology, 97: 417~430.

Davidson J P. 1987. Crustal contamination versus subduction zone enrichment: examples from the Lesser Antilles and implications for mantle source compositions of island arc volcanic rocks[J]. Geochimica et Cosmochimica Acta, 51(8): 2 185~2 198.

Engebretson D C, Cox A and Gordon R G. 1985. Relative motions between oceanic and continental plates in the pacific basin[J]. Geological Society of America, Special Publications, 206: 1~59.

Ernst W G, Tsujimori T, Zhang R, *et al*. 2007. Permo-Triassic collision, subduction-zone metamorphism, and tectonic exhumation along the East Asian continental margin[J]. Annual Review of Earth and Planetary Sciences, 35: 73~110.

Ewart A. 1982. The mineralogy and petrology of Tertiary-Recent orogenic volcanic rocks: With special reference to the andesitic-basaltic compositional range[A]. Andesites: Orogenic Andesites and Related Rocks[C]. New York: John Wiley and Sons, 25~95.

Feng Guangying, Liu Shen, Niu Xiaolu, *et al*. 2018. Geochronology, geochemistry and petrogenesis of Early-Middle Permian mafic intrusion in Zhangguangcai Range, China[J]. Earth Science, 43(4): 1 293~1 310(in Chinese with English abstract).

Fitton J G, James D, Kempton P D, *et al*. 1988. The role of lithospheric mantle in the generation of late Cenozoic basic magmas in the western United States[J]. Journal of Petrology, Special Volume (1): 331~349.

Fukuyama M, Ogasawara M, Horie K, *et al*. 2013. Genesis of jadeite-quartz rocks in the Yorii area of the Kanto Mountains, Japan[J]. Journal of Asian Earth Sciences, 63: 206~217.

Ge Maohui, Zhang Jinjiang and Liu Kai. 2020. Geochronology, geochemistry and zircon Hf isotope of the Jurassic diabase from the Tieli area, Lesser Xing'an-Zhangguangcai Range, and its geological implications [J]. Acta Petrologica Sinica, 36(3): 726~740(in Chinese with English abstract).

Gill J B. 1981. Orogenic Andesites and Plate Tectonics[M]. Berlin: Springer-Verlag, 1~385.

Guo Feng. 2016. Geological records of the Pacific Plate subduction in the northeast Asian continental margin: An overview[J]. Bulletin of Mineralogy, Petrology and Geochemistry, 35(6): 1 082~1 089(in Chinese with English abstract).

Guo F, Li H X, Fan W M, *et al*. 2015. Early Jurassic subduction of the Paleo-Pacific Ocean in NE China: Petrologic and geochemical evidence from the Tumen mafic intrusive complex[J]. Lithos, 224~225: 46~60.

Hanyu T, Tatsumi Y, Nakai S, *et al*. 2006. Contribution of slab melting and slab dehydration to magmatism in the NE Japan arc for the last 25 Myr: Constraints from geochemistry[J]. Geochemistry, Geophysics, Geosystems, 7(8): 1~29.

Leat P T, Riley T R, Wareham C D, *et al*. 2002. Tectonic setting of primitive magmas in volcanic arcs: An example from the Antarctic Peninsula[J]. Journal of the Geological Society of London, 159: 31~44.

Liati A, Gebauer D and Wysoczanski R. 2002. U-Pb SHRIMP-dating of zircon domains from UHP garnet-rich mafic rocks and late pegmatoids in the Rhodope zone (N Greece): Evidence for Early Cretaceous crystallization and Late Cretaceous metamorphism[J]. Chemical Geology, 184: 281~299.

Liu J, Liu Z H, Zhao C, *et al*. 2017. Geochemistry and U-Pb detrital zircon ages of late Permian to Early Triassic metamorphic rocks from northern Liaoning, North China: Evidence for the timing of final closure of the Paleo-Asian Ocean[J]. Journal of Asian Earth Sciences, 145: 460~474.

Liu Jinlong, Sun Fengyue, Wang Yingde, *et al*. 2016. Tectonic setting of Hadahushu mafic intrusion in Urad Zhongqi Area, Inner Mongolia: Implications for Early subduction history of Paleo-Asian Ocean Plate [J]. Earth Science, 41(12): 2 019~2 030(in Chinese with English abstract).

Ma X H, Zhu W P, Zhou Z H, *et al*. 2017. Transformation from Paleo-Asian Ocean closure to Paleo-Pacific subduction: New constraints from granitoids in the eastern Jilin-Heilongjiang Belt, NE China[J]. Journal of Asian Earth Sciences, 144: 261~286.

Maniar P D and Piccoli P M. 1989. Tectonic discrimination of granitoids [J]. Geological Society of America Bulletin, 101: 635~643.

Meng E, Xu W L, Pei F P, *et al*. 2011. Permian bimodal volcanism in the Zhangguangcai Range of eastern Heilongjiang Province, NE China: Zircon U-Pb-Hf isotopes and geochemical evidence[J]. Journal of Asian Earth Sciences, 41: 119~132.

Miyashiro A. 1974. Volcanic rock series in island arcs and active continental margin[J]. American Journal of Science, 274: 321~335.

Pearce J A. 2008. Geochemical fingerprinting of oceanic basalts with applications to ophiolite classification and the search for Archean oceanic crust[J]. Lithos, 100(1): 14~48.

Pearce J A, Harris N B W and Tindle A G. 1984. Trace element discrimination diagrams for the tectonic interpretation of granitic rocks[J]. Journal of Petrology, 25: 956~983.

Pei Fuping, Xu Wenliang, Yang Debin, *et al*. 2008. Mesozoic volcanic rocks in the southern Songliao basin: Zircon U-Pb ages and their constraints on the nature of basin basement[J]. Earth Science, 33(5): 603~617(in Chinese with English abstract).

Ridolfi F, Renzulli A and Puerini M. 2010. Stability and chemical equilibrium of amphibole in calc-alkaline magmas: An overview, new thermobarometric formulations and application to subduction-related volcanoes [J]. Contributions to Mineralogy and Petrology, 160: 45~66.

Safonova I Y and Santosh M. 2014. Accretionary complexes in the Asia-Pacific region: Tracing archives of ocean plate stratigraphy and tracking mantle plumes[J]. Gondwana Research, 25: 126~158.

Saunders A D, Storey M, Kent R W, *et al*. 1992. Consequences of plume-lithosphere interactions [J]. Geological Society, London, Special Publications, 68: 41~60.

Sun Deyou, Wu Fuyuan, Gao Shan, *et al*. 2005. Confirmation of two episodes of A-type granite emplacement during Late Triassic and Early Jurassic in the central Jilin Province, and their constraints on the structural pattern of Eastern Jilin-Heilongjiang Area, China [J]. Earth Science Frontiers, 12(2): 263~275(in Chinese with English abstract).

Sun M D, Xu Y G, Wilde S A, *et al*. 2015. The Permian Dongfanghong island-arc gabbro of the Wandashan Orogen, NE China: Implications for Paleo-Pacific subduction[J]. Tectonophysics, 659: 122~136.

Sun S S and McDonough W F. 1989. Chemical and isotopic systematics of oceanic basalts: Implications for mantle composition and processes [J]. Geological Society, London, Special Publications, 42(1): 313~345.

Sun Y G, Li B L, Sun F Y, *et al*. 2020. Geochronology, geochemistry, and Hf isotopic compositions of Early Permian syenogranite and diabase from the northern Great Xing'an Range, NE China: Petrogenesis and tectonic implications[J]. Canadian Journal of Earth Sciences, 57(12): 1 478~1 491.

Tang J, Xu W L, Wang F, *et al*. 2018. Subduction history of the Paleo-Pacific slab beneath Eurasian continent: Mesozoic-Paleogene magmatic records in Northeast Asia[J]. Science China (Earth Sciences), 61(5): 527~559.

Tang J, Xu W L, Wang F, *et al*. 2016. Early Mesozoic southward subduction history of the Mongol-Okhotsk oceanic plate: Evidence from geochronology and geochemistry of Early Mesozoic intrusive rocks in the Erguna Massif, NE China[J]. Gondwana Research, 31: 218~240.

Thompson R N and Morrison M A. 1988. Asthenospheric and lower-lithospheric mantle contributions to continental extensional magmatism: An example from the British Tertiary Province[J]. Chemical Geology, 68(1~2): 1~15.

Tomaschek F, Kennedy A K, ViHa I M, *et al*. 2003. Zircons from Syros, Cyclades, Greece-recrystallization and mobilization of zircon during high-pressure metamorphism[J]. Journal of Petrology, 44(11): 1 977~2 002.

Wang F, Xu W L, Xing K C, *et al*. 2019. Final closure of the Paleo-Asian Ocean and onset of subduction of Paleo-Pacific Ocean: Constraints from early Mesozoic magmatism in central southern Jilin Province, NE China[J]. Journal of Geophysical Research: Solid Earth, 124(3): 2 601~2 622.

Wang F, Xu Y G, Xu W L, *et al*. 2017. Early Jurassic cal-calkaline magmatism in northeast China: magmatic response to subduction of the Paleo-Pacific Plate beneath the Eurasian continent[J]. Journal of Asian Earth Sciences, 143: 249~268.

Wang Guan, Sun Fengyue, Li Bile, *et al*. 2014. Petrography, zircon U-Pb geochronology and geochemistry of the mafic-ultramafic intrusion in Xiarihamu Cu-Ni deposit from East Kunlun, with implications for geodynamic setting[J]. Earth Science Frontiers, 21(6): 381~401(in Chinese with English abstract).

Wang Y N, Xu W L, Wang F, *et al*. 2018. New insights on the early Mesozoic evolution of multiple tectonic regimes in the northeastern North China craton from the detrital zircon provenance of sedimentary strata[J]. Solid Earth, 9(6): 1 375~1 397.

Wang Z J, Xu W L, Pei F P, *et al*. 2015. Geochronology and geochemistry of middle Permian-middle Triassic intrusive rocks from central-eastern Jilin Province, NE China: Constraints on the tectonic evolution of the eastern segment of the Paleo-Asian Ocean[J]. Lithos, 238: 13~25.

Wilde S A. 2015. Final amalgamation of the Central Asian Orogenic Belt in NE China: Paleo-Asian Ocean closure versus Paleo-Pacific plate subduction—a review of the evidence[J]. Tectonophysics, 662: 345~362.

Wilson M. 1989. Review of igneous petrogenesis: A global tectonic approach[J]. Terra Nova, 1(2): 218~222.

Wu Fuyuan, Li Xianhua, Zheng Yongfei, *et al*. 2007. Lu-Hf isotopic systematics and their applications in petrology[J]. Acta Petrologica Sinica, 23(2): 185~220(in Chinese with English abstract).

Wu F Y, Sun D Y, Ge W C, *et al*. 2011. Geochronology of the Phanerozoic granitoids in northeastern China[J]. Journal of Asian Earth Sciences, 41: 1~30.

Wu F Y, Yang Y H, Xie L W, *et al*. 2006. Hf isotopic Compositions of the Standard Zircons and Baddeleyites used in U-Pb Geochronology [J]. Chemical Geology, 234(1): 105~126.

Wu F Y, Zhao G C, Sun D Y, *et al*. 2007. The Hulan Group: Its role in the evolution of the Central Asian Orogenic Belt of NE China[J]. Journal of Asian Earth Sciences, 30: 542~556.

Wu Y B and Zheng Y F. 2004. Genesis of zircon and its constraints on interpretation of U-Pb age[J]. Chinese Science Bulletin, 49(15): 1 554~1 569.

Xu W L, Pei F P, Wang F, *et al*. 2013. Spatial-temporal relationships of Mesozoic volcanic rocks in NE China: Constraints on tectonic overprinting and transformations between multiple tectonic regimes[J]. Journal of Asian Earth Sciences, 74: 167~193.

Yan Jiaming, Sun Fengyue, Chen Guangjun, *et al*. 2016. Geochemical characteristics of gabbro from Binggounan Cu-Ni deposit in the north of eastern Kunlun metallogenic belt[J]. Global Geology, 35(3): 729~737(in Chinese with English abstract).

Yan J M, Sun F Y, Li B L, *et al*. 2020. Geochronological, geochemical, and mineralogical characteristics of the Akechukesai-I mafic-ultramafic complex in the eastern Kunlun area of the northern Tibet Plateau, west China: Insights into ore potential[J]. Ore Geology Reviews, 121: 103 468.

Yan J M, Sun F Y, Li L, *et al*. 2019. A slab break-off model for mafic-ultramafic igneous complexes in the East Kunlun Orogenic Belt, northern Tibet: Insights from early Palaeozoic accretion related to post-collisional magmatism[J]. International Geology Review, 61(10): 1 171~1 188.

Yang H, Ge W C, Zhao G C, *et al*. 2015. Early Permian-Late Triassic granitic magmatism in the Jiamusi-Khanka Massif, eastern segment of the Central Asian Orogenic Belt and its implications[J]. Gondwana Research, 27: 1 509~1 533.

Yang J H, Wu F Y, Shao J A, *et al*. 2006. Constrains on the timing of uplift of the Yanshan Fold and Thrust Belt, north China[J]. Earth and Planetary Science Letters, 246: 336~352.

Yang Zeli, Wang Shuqing, Hu Xiaojia, *et al*. 2018. Geochronology and geochemistry of Early Paleozoic gabbroic diorites in East Ujimqin Banner of Inner Mongolia and their geological significance[J]. Acta Petrologica et Mineralogica, 37(3): 349~365(in Chinese with English abstract).

Yu J J, Wang F, Xu W L, *et al*. 2012. Early Jurassic mafic magmatism in the Lesser Xing'an-Zhangguangcai Range, NE China, and its tectonic implications: Constraints from zircon U-Pb chronology and geochemistry[J]. Lithos, 142~143: 256~266.

Zhang Y Y, Yuan C, Sun M, *et al*. 2015. Permian doleritic dikes in the Beishan Orogenic Belt, NW China: Asthenosphere-lithosphere interaction in response to slab break-off[J]. Lithos, 233: 174~192.

Zhao Chunjing, Peng Yujing, Dang Zengxin, *et al*. 1996. The Structural Framework and Crustal Evolution in Eastern Jilin and Heilongjiang Provinces[M]. Shenyang: Liaoning University Press, 1~186 (in Chinese with English abstract).

Zhao L, Guo F, Fan W M, *et al*. 2019. Roles of subducted pelagic and terrigenous sediments in Early Jurassic mafic magmatism in NE China: Constraints on the architecture of Paleo-Pacific subduction zone[J]. Journal of Geophysical Research: Solid Earth, 124(3): 2 525~2 550.

Zhong S H, Feng C Y, Seltmann R, *et al*. 2017. Middle Devonian volcanic rocks in the Weibao Cu-Pb-Zn deposit, East Kunlun Mountains, NW China: Zircon chronology and tectonic implications[J]. Ore Geology Reviews, 84: 309~327.

Zhou J B, Wilde S A, Zhang X Z, *et al*. 2009. The onset of Pacific margin accretion in NE China: Evidence from the Heilongjiang high-pressure metamorphic belt[J]. Tectonophysics, 478: 230~246.

附中文参考文献

奥 琮, 孙丰月, 李碧乐, 等. 2015. 东昆仑祁漫塔格地区小尖山辉长岩地球化学特征、U-Pb年代学及其构造意义[J]. 大地构造与成矿学, 39(6): 1 176~1 184.

冯光英, 刘 燊, 牛晓露, 2018. 张广才岭地块早-中二叠世镁铁质侵入岩体的年代学、地球化学及岩石成因[J]. 地球科学, 43(4): 1 293~1 310.

葛茂卉, 张进江, 刘 恺. 2020. 小兴安岭-张广才岭铁力地区侏罗纪辉绿岩年代学、地球化学、锆石Hf同位素特征及其构造意义[J]. 岩石学报, 36(3): 726~740.

郭 锋. 2016. 太平洋板块俯冲作用在东北亚大陆边缘的地质记录评述[J]. 矿物岩石地球化学通报, 35(6): 1 082~1 089.

刘金龙, 孙丰月, 王英德, 等. 2016. 内蒙古乌拉特中旗哈达呼舒基性岩体形成的构造背景与古亚洲洋的早期俯冲历史[J]. 地球科学, 41(12): 2 019~2 030.

裴福萍, 许文良, 杨德彬, 等. 2008. 松辽盆地南部中生代火山岩: 锆石U-Pb年代学及其对基底性质的制约[J]. 地球科学, 33(5): 603~617.

孙德有, 吴福元, 高 山, 等. 2005. 吉林中部晚三叠世和早侏罗世两期铝质A型花岗岩的厘定及对吉黑东部构造格局的制约[J]. 地学前缘, 12(2): 263~275.

王 冠, 孙丰月, 李碧乐, 等. 2014. 东昆仑夏日哈木铜镍矿镁铁质-超镁铁质岩体岩相学、锆石U-Pb年代学、地球化学及其构造意义[J]. 地学前缘, 21(6): 381~401.

吴福元, 李献华, 郑永飞, 等, 2007. Lu-Hf同位素体系及其岩石学应用[J]. 岩石学报, 23(2): 185~220.

闫佳铭, 孙丰月, 陈广俊, 等. 2016. 东昆北成矿带冰沟南铜镍矿辉长岩地球化学特征[J]. 世界地质, 35(3): 729~737.

杨泽黎, 王树庆, 胡晓佳, 等. 2018. 内蒙古东乌珠穆沁旗早古生代辉长闪长岩年代学和地球化学特征及地质意义[J]. 岩石矿物学杂志, 37(3): 349~365.

赵春荆, 彭玉鲸, 党增欣, 等. 1996. 吉黑东部构造格架及地壳演化[M]. 沈阳: 辽宁大学出版社, 1~186.